Reduced-order optimal interpolation for biomass assimilation

G. Crispi, M. Pacciaroni, D. Viezzoli

Ocean Sci. Discuss., 3, 503–539, 2006
www.ocean-sci-discuss.net/3/503/2006/

Papers published in *Ocean Science Discussions* are under
open-access review for the journal *Ocean Science*

Reduced-order optimal interpolation for biomass assimilation

G. Crispi, M. Pacciaroni, and D. Viezzoli

Istituto Nazionale di Oceanografia e di Geofisica Sperimentale, Italy

Received: 31 March 2006 – Accepted: 30 April 2006 – Published: 19 June 2006

Correspondence to: G. Crispi (gcrispi@ogs.trieste.it)

Abstract

The analysis of the evolution of the chemical and biological characteristics of the Mediterranean marine ecosystem requires an integrated approach. Consistently, an ecosystem description, embedded in the MFSTEP one eighth degree three-dimensional general circulation model, is tested and used following a twin experiment approach. The ecosystem model is based on the NPZD trophic chain: inorganic nitrogen, N, phytoplankton, P, zooplankton, Z and detritus, D. Assimilation of synthetic biomass data is performed by means of the reduced-order optimal interpolation system SOFA.

The synthetic "sea-truth" data are daily averages obtained from a sixty-nine days reference run (RR). The twin experiments consist in performing two runs: a free run (FR) with wrong summer-depleted phytoplankton initial conditions and an assimilated run (AR), in which, starting from the same FR wrong phytoplankton concentrations, weekly averaged surface biomasses extracted from the RR results are assimilated.

The comparison of the FR results with the AR ones shows a good convergence, on a basin Mediterranean scale, confirming improvements of the forecasting in each of the four ecological compartments.

Regional trophic regimes are analysed and interpreted in the western and eastern Mediterranean subbasins, for explaining the deteriorating behaviour of the total nitrogen.

1 Introduction

The last two decades of the twentieth century saw the development of remote sensing techniques to study the distribution of phytoplankton in the ocean. This technology uses subtle variations in the color of the oceans, as monitored by a sensor aboard satellites, to quantify variations in the concentration of chlorophyll-a in the surface layers of the ocean. Since polar-orbiting satellites' swaths cover the globe at high spatial

OSD

3, 503–539, 2006

resolution – 1 km or better), it is possible to see in great wealth of detail the variations in phytoplankton distribution at synoptic scales. The next logical step in the exploitation of ocean-color data was taken a few years later, when these fields of biomass were converted into fields of primary production. On this innovations are based the improvements of models describing photosynthesis as a function of available light.

The aim of this work is to evaluate the feasibility, the efficiency and the limits of the assimilation of superficial biomass data in view of possible activities in operational oceanography. Assessing the potential improvement of basin scale ecosystem predictions for the Mediterranean Sea adopting data assimilation strategies for ocean colour data is the theme of a companion research. The Observing System Simulation Experiment proposed here provide the quantitative basis for a rationale design of subsurface observing systems that have to complement the information from the satellite ocean colour.

The procedure which can meet the most success relies on models of the photosynthesis as a function of the photosynthetic available radiation and of the nutrient cycling. Thus the light available at the sea surface is estimated in this work using optimization methods, and the nitrogen limitation is traced as discussed in the following.

The numerical experiment is based upon an established ecosystem model set up in the frame of the European Commission Mediterranean Targeted Projects 1 (Pinardi et al., 1997) and 2 (Monaco and Peruzzi, 2002). The model has moderated biological complexity to be used in tight coupling with the assimilation scheme. Moreover there is experience that such a model can capture the main biogeochemical fluxes characteristics of the Mediterranean basin: oligotrophy, seasonal cycle, biological gradients.

In the frame of the study of the interaction among hydrodynamical processes and ecological systems, a quantitative interpretation of the biogeochemical processes in the Ionian Sea and of the seasonal variability of the nitrogen cycles in Mediterranean has been gained. In the Ionian Sea the trophic web is dominated by the nutrient regeneration. This mechanism releases the dissolved organic phase in the inorganic one, which is immediately reusable by primary living organisms. Results of the Ionian

model are taken after spin-up of the hydrodynamics forty-five months long (Civitarese et al., 1996). In this study, the initialization was based on the chemical data gathered during the cruise POEM-BC-O91, while the biology was initialized with an average of measured profiles. As a result, the dynamics of phytoplankton depended both on the nitrogen flux coming from the Sicily Strait and on the vertical movements due to gyres and upwelling. Estimate of the primary production was in good accord with the one obtained on the basis of consumed oxygen. The climatological influence of the general circulation on the nutrient distribution was evident in permanent cyclonic areas, while anticyclonic areas did not give valuable signals because of the high oligotrophy of the superficial layer.

Thus basic trophodynamics coupled with the general circulation reproduces biological and ecological main features of the oligotrophic marine environment like Ionian subbasin. In the present work a similar approach is followed maintaining fixed properties and characteristic parameters of plankton, while the available nitrogen is the only free environmental nutrient.

In the following section the integrated system set-up is outlined. The dynamical adjustment of the initial conditions is considered in the third section, while in the fourth one the results in terms of overall content in the different ecosystem compartments and their statistics are shown. The last section summarizes the conclusions.

2 Ecological model set up

The dynamic of the Mediterranean oligotrophic ecosystem is studied through coupling with the Mediterranean basin circulation as simulated by General Circulation Model driven by high frequency forcing. Consistently, ecosystem description concerning the general circulation with three-dimensional models has been set up according with the implementation obtained during the Mediterranean Forecasting System Project (Demirov and Pinardi, 2002).

Specifically, the simulations reported here adopt a GCM for the Mediterranean Sea

plus a buffer zone representing the Atlantic inflow/outflow. Air-sea physical parameterizations account for the heat budget at the air-sea interface using sea surface temperature prognosed by the model. Six-hourly atmospheric fields from European Centre for Medium-Range Weather Forecast – ECMWF are used. The biharmonic horizontal eddy viscosity is $0.5\times10^{18}\,cm^4\,s^{-1}$ and the biharmonic horizontal eddy diffusivity is $1.5\times10^{18}\,cm^4\,s^{-1}$ for physical tracers. The vertical viscosity is $1.5\,cm^2\,s^{-1}$, the vertical diffusivity for temperature and salinity is $0.3\,cm^2\,s^{-1}$.

The model is integrated throughout all the Mediterranean basin, with horizontal spatial discretization of one eighth degree and with vertical resolution of 31 levels. On the same grid the equations describing nitrogen uptake, grazing and remineralization processes, are integrated. The vertical levels are unevenly spaced down to 4000 m, and the tracer values, temperature, salinity and biochemical ones, biomass among the others, are placed at 5, 15, 30, 50, 70, 90, 120, 160, 200, 240, 280, 320, 360, 400, 440, 480, 520, 580, 660, 775, 925, 1150, 1450, 1750, 2050, 2350, 2650, 2950, 3250, 3550, 3850 m.

The specification of salt fluxes at surface is obtained with the relaxation of model sea surface salinity toward climatological casts for the Mediterranean area. Convective adjustment is performed mixing the contents of two adjacent vertical levels, when static instability occurs.

The biological variations of the dissolved inorganic carbon concentration in the sea are relatively small and difficult to detect against high background values. Thus this ecosystem model is based on nitrogen units.

Firstly, a reciprocal interaction between the elemental composition of marine biota and their dissolved nutrition resources is assumed, whereby the nutrient elements are taken up and released in fixed proportions of C:N:P of 106:16:1 (Redfield et al., 1963). Secondly, the biological production is principally limited by the availability of nitrogen, meaning that the supply of nitrogen also determines the amount of carbon incorporated into biomass. Production based on nitrogen (e.g. nitrate), which newly enters the euphotic zone, where light availability is sufficient for net growth, is referred to as

new production and is differentiated from production based on the remineralized compounds of nitrogen. Accordingly, the export flux of organic material from this upper oceanic layer equals the new production.

The aim of simulating relevant biological processes of the nitrogen cycle has led to the development of relatively simple nitrogen-based models of marine ecosystems. One could argue whether these models really simulate ecosystems or should rather be named biogeochemical models. That is, because such models simply transfer mass from an inorganic reservoir into organic pools and may lack, for instance, important ecological processes. Nevertheless, the terminology "ecosystem model" is commonly used for those biological models that include parameterisations mostly describing mass exchange rates. In general the model parameters are considered to be constant in time. Hence, the model solutions strongly depend on the choice of the corresponding biological parameters which, in addition, need to represent a diversity of individual organisms, grouped into compartments of, for example, phytoplankton and herbivorous zooplankton. Since the model parameters should represent a complex system in such a simple way, their appropriate estimate remains a major challenge.

Here the basic equations of the NPZD nitrate-based model are presented, see Fig. 1. The three-dimensional coupling of generic equation of the biological tracer BT with sea velocity field $\bar{u}=(u, v, w)$ is:

$$\frac{\partial \mathrm{BT}}{\partial t} + (\bar{u} \cdot \nabla)\mathrm{BT} = -K_H \nabla_H^4 \mathrm{BT} + K_V \frac{\partial^2 \mathrm{BT}}{\partial z^2} - w_{\mathrm{BT}} \frac{\partial \mathrm{BT}}{\partial z} + \left.\frac{\partial \mathrm{BT}}{\partial t}\right|_{\mathrm{SOURCE}}$$

with hydrodynamics and its parameterization on the same grid of the Mediterranean circulation model, where the equations describing nitrogen uptake, grazing and remineralization processes, are integrated. Every variable has a positive flux to the following: the uptake from nitrate to phytoplankton; the grazing from phytoplankton to detritus; the mortality from zooplankton to detritus; and the remineralization from detritus to nitrate. Also the specific lysis from phytoplankton to detritus is shown. These five fundamental fluxes are completed by the cross fluxes from zooplankton to nitrate, the excretion, and from phytoplankton to detritus, the sloppy feeding.

Biogeochemical equations, without any recourse to boundary conditions inside the integration domain, are solved in insulating, conservative way through second-order finite difference method on the numerical B-grid, at the time step of 900 s (15 min). When instabilitites occur in the biogeochemistry, biological sources and sinks are set to zero and the calculations proceed after borrowing.

The nitrogen model gives the space and time evolution of nitrate, N, phytoplankton, P, zooplankton, Z, detritus, D, all in nitrogen units. The phytoplankton equation is given by the following expression:

$$\left.\frac{\partial \mathrm{P}}{\partial t}\right|_{\mathrm{SOURCE}} = G(t)\frac{\mathrm{NP}}{k_N + \mathrm{N}} - d\ \mathrm{P} - \gamma\frac{\mathrm{P\ Z}}{k_P + \mathrm{P}}$$

Growth limitation, $G(t)$, is described by the Eppley (1972) function:

$$G(t) = G_{\max} e^{-k_T T} E(I, I_{\mathrm{opt}}, z, t)$$

with

$$E(I, I_{\mathrm{opt}}, z, t) = p(t)\frac{I}{I_{\mathrm{opt}}} e^{1-(I/I_{\mathrm{opt}})}$$

Here the limitation by photosynthetic available radiation is given in terms of the photoperiod in the julian day, p(t), of the $\mathrm{I_{opt}}$ optimum light irradiance, and of the irradiance, I, at z depth:

$$I = I_0(t) e^{-k_z z}$$

expressed as function of the irradiance at surface optimized following data by Sverdrup at al. (1942) using the Beers (1966) light extinction law.

Grazing activity is expressed in order to introduce sloppy feeding and excretion:

$$\left.\frac{\partial \mathrm{Z}}{\partial t}\right|_{\mathrm{SOURCE}} = \eta\gamma\frac{\mathrm{PZ}}{k_P + \mathrm{P}} - \delta\ \mathrm{Z}$$

The nitrate takes into account all the other biochemical variables as follows:

$$\left.\frac{\partial \mathrm{N}}{\partial t}\right|_{\mathrm{SOURCE}} = r\ D + (1-\alpha)\delta\ Z - G\frac{\mathrm{N}\ \mathrm{P}}{k_N + \mathrm{N}}$$

The detritus chain describes the remaining part of the biogeochemical cycles of carbon and macronutrients, that is the recycling, through mineralization, of the nonliving organic matter, particulate and dissolved, produced by exogenous input, mortality processes, excretion and exudation, all set as linear processes. The introduction of the detritus compartment permits to follow the fate and the remineralization of the particulate matter at a basin and sub-basin scale below the euphotic zone, which are conditions for balancing the new production:

$$\left.\frac{\partial D}{\partial t}\right|_{\mathrm{SOURCE}} = d\ P + (1-\eta)\gamma\ \frac{\mathrm{PZ}}{k_P + \mathrm{P}} + \alpha\,\delta\ \mathrm{Z} - r\ \mathrm{D}$$

All the parameters are chosen in literature ranges for oligotrophic environments (Table 1). This enables to calibrate, considering selected results from MTP I and MTP II Projects, the 3-D model to the values of detritus remineralization and sinking.

The univariate version 3.0 of System for Ocean Forecast and Analysis (SOFA) by De Mey and Benkiran (2002) is used for assimilating surface biomass data. SOFA, using temperature and salinity as tracers (Raicich and Rampazzo, 2003), has been ported from SGI ORIGIN to IBM-SP4-AIX 5.1 with 48 nodes, 512 POWER 4 1.3 GHz CPU's, 1088 GB RAM.

The NPZD model is embedded in the integrated system, hydrodynamics plus ecology plus optimal interpolation. This new version, after debugging and optimization, is tested in numerical experiments. To this aim procedures and compiler options are added and modified in GCM and in SOFA to introduce assignements, time-run evaluations, and system supported functions consistent with the ecological application and with the hardware. The required ESSL and LAPACK libraries are substituted with the optimized MASS library.

After optimization of the cache and introducing the order O2 compiler f77 the execution time is reduced approximately by three from about 600 to 227 s for one day simulation with time-step of 900 s.

3 Initial conditions dynamical adjustment

Phytoplankton initial conditions are chosen from the data of an averaged summer profile. Averaged biomass stations were measured by Berland et al. (1988; see Fig. 5) in the Balearic Sea, in the Ionian Sea and in the Levantine. A ratio of 0.05 for estimating the chlorophyll to carbon is used. The profile is shown in Fig. 2, inner panel. Zooplankton is initialized as one ninth of the phytoplankton value, i.e. around 11–12% of the total phytoplankton content.

Mean nitrate summer conditions are extracted from the MEDAR climatology (Manca et al., 2004). Areas DS4, DJ7, DH3 are selected and averaged, in correspondence to analogous regions in which phytoplankton data were acquired. The interpolation at the depth of the model is reported in Fig. 2, large panel. This profile initializes nitrate variable for all the Mediterranean basin.

Atlantic Ocean and marginal seas, Adriatic and Aegean, influences upon the pelagic Mediterranean Sea are treated using historical data (Fig. 2).

Initialisation and restoring to the same values of the Atlantic Ocean are performed for obtaining nitrogen fluxes in keeping with various different estimates. The station data are selected from the ATLANTIS II cruise report (Osborne et al., 1992). The reference latitude is 36.5° N and the longitude of these casts range from 9.5° W to 8° W.

Atlantic and Gibraltar restoring condition are included from 9.25° W to 6.00° E.

For the Middle Adriatic Sea, a profile which averages the mean biochemical climatological values is selected, taking into account the main effects of the rivers and of the shelf processes. These climatological profiles do maintain a strong stability in the water column during the seasonal cycles (Zavatarelli et al., 1998; particularly in Fig. 11 dedicated to the seasonal vertical profiles in the Middle Adriatic). To this aim, a cen-

tral box of the Adriatic Sea northerly than 43° N is averaged. All the casts between Rimini-Pula and Vieste-Split transects are selected, but only if deeper than 80 m.

This marginal region begins at 12° E and ends at 18° E, from the latitude 43° N. Middle Adriatic nitrate vertical profile at 43° N is shown in Fig. 2.

For the Aegean Sea, a full box including the Cretan Sea northerly than 38° N is considered starting from measured profiles (McGill, 1970). In this northern marginal area it is convenient to take into account the fluxes through the Aegean, in view of studies about climatic changes in the pelagic southern and deeper area. This second marginal region begins at 22° E and ends at 28° E, from 38° N. Potential temperature and salinity are not restored to climatological values, instead of the procedures in effect at Gibraltar and in the Middle Adriatic. Aegean nitrate vertical profile at 38° N is reported in Fig. 2. Moreover, detritus is set from surface to 100 m depth to the 0.5 μmol N dm^{-3} initial condition; the value is null beneath. This accords with Coste et al. (1988) particulate matter, as measured in the inflowing Atlantic water.

Atmospheric loads and terrestrial inputs are set to zero at this stage of the system application. Some considerations about different inputs strategies are discussed in the following section, estimating total inorganic loads, going completely into inorganic nitrogen, and fractionated ones, i.e. inputs divided between dissolved inorganic nitrogen (50%) and detritus (50%).

The following sequence shows the evolution of the phytoplankton at surface. In the middle of the preconditioning period, 30 October snapshot, the phytoplankton generally increases in the 20 m upper layer, Fig. 3. Starting from the initial homogeneous value of 0.0144 μmol N dm^{-3}, biomass in terms of nitrogen reaches its highest concentration values in the Alboran Sea, in the Gulf of Lions, in Sardinia and Sicily upwelling areas, in the Sirte Gulf and along Egyptian coast. These maxima are generally higher than the initial conditions.

Nitrate at the same depth, not shown, is generally depleted toward values of about 0.05 μmol N dm^{-3}, presenting clear negative anomalies with respect to the starting value 0.0845. In the Gulf of Lions and in the other eutrophic areas high values of nutri-

ent and of biomass coexist. It is in progress a late summer evolution from homogenous values toward nutrient gradients, decreasing from west to east in the different sub-basins of the Mediterranean.

In Fig. 4 the surface phytoplankton concentration is shown after 120 days, on 29 December, at the beginning of the reference run. Biomass increase is evident in this pre-bloom period in a vast area of the western basin. The biomass maxima reach values about 0.2 μmol N dm^{-3}, more than ten times summer initial concentration.

After 120 days, inorganic nitrogen, not shown, is analogously at high values corresponding to the maxima in biomass at Fig. 4. The nutrient-rich sites are the Alboran Sea, Ligurian-Provencal and Tyrrhenian Seas, large parts of Adriatic and Aegean, coastal areas along the African coast in the eastern basin.

The surface velocities, not shown, at the same depth show weakening of the anticyclonic characteristics of the late summer situation toward the winter one (Alboran Sea, southern Ionian, far Eastern Mediterranean). The along-shore currents intensify in these two months in the Gulf of Lions and Tyrrhenian coast; with the formation of cyclonic gyres or their intensification, if permanent.

4 Twin experiment results and discussion

The twin experiment starts from the results of the dynamical adjustment run discussed before. The forcing functions are the daily forcing of the year 1998. All the three runs start on 29 December and, after reaching the end of the year, they continue with the 1 January till the 7 March forcings of the same year, see Fig. 5.

The reference run starts from the final conditions of the dynamical adjustment. No assimilation is performed. The free run starts from the final conditions of the dynamical adjustment run for all variables except phytoplankton, reinitialized to summer initial conditions and no assimilation is performed. Also the assimilation run starts from the wrong initial conditions of the free run. However the weekly data of phytoplankton, as averaged from the daily results of the reference run, are assimilated.

Figure 6 shows the data flow between SOFA and MOM. Nine files are created as input assimilation data, each with the weekly average of the biomass to be assimilated at the end of the corresponding week in the two upper levels, at 5 and 15 m. These files contain estimates of the standard deviation of the biomass; row information with the identificator of the file, the longitude, the latitude, the time – in our case data are given at the end of the week – i.e. 7 days, 14 days, etc., and the number of measures – each profile is made of two data, the first for the upper 10 m level and the second for the adjacent subsurfacial 10 m level. The standard data loader reads univariate vertical profile data.

At the beginning, the 41 019 vertical profiles are read one for each grid point; after this input, SOFA performs preprocessing of MVS format, packed Multivariate Vertical Sequence, at each grid point and every week, and records it in the SOFA database.

When the system needs the stored vertical profiles, it searches vertical profiles records in SOFA database in line with the windowing cycle and stores their data unit pointers for current three-dimensional analysis.

Control is performed giving the vertical data number, NMVS, for each model sea point and the vector containing the indices of data for that superficial point. The first represents the length of reduced MVS; the second is the reduced MVS. Then SOFA computes corrections in packed MVS form.

At the end, and this completes assimilation cycle shown in Fig. 6, correction is calculated in GCM using SOFA input.

The evolution of the phytoplankton is shown in Fig. 7a. The three basin averages – of the Reference Run (non-assimilated and imperturbed run – RR), of the Free Run (non assimilated and re-initialized with summer biomass – FR), of the Assimilation Run (assimilated and re-initialized with summer biomass – AR) are followed during the sixty-nine days of the evolution. In the RR, total phytoplankton increases from the initial value, reached at the end of the adjustment period, toward higher values, and, after these maxima obtained at the end of the bloom, it decreases.

The FR gives a completely different behaviour: starting from quite low values, due to

the summer biomass conditions injected at the beginning of the run, it has a very fast step in the first 40 days towards maxima of the same order in the RR; at the end of the sixty-nine days period, distinct higher values are attained.

In the AR, the steps toward maxima every seven days, i.e. at assimilation times, are more pronounced than in FR, getting facilities from the optimal interpolation procedure; in every case, at the end of the twin experiment lower values than FR ones are reached. Thus the assimilating evolution is closer to the "sea-truth" biomass response than the free one.

AR zooplankton behaviour (Fig. 7b) is very close to the free one, even if only phytoplankton biomass is assimilated in our experiment. At the end of the simulation the former remains closer to the RR response than the latter.

Inorganic nitrogen, detritus and total nitrogen (sum of the four compartments) are given in Fig. 8. In the inorganic nitrogen plate (Fig. 8a), a more complex pattern is evidenced. This is because there is a strong beginning uptake in the reference run, with respect to free and assimilation ones, for the great biomass due to the initial conditions. After 30 days inorganic nitrogen is greater in the reference, for the sum of two reasons: the higher uptake experienced in the other two runs, and the missing part of the initial biomass that influences the lower values.

As the last compartment, the detritus shows very low values in FR and AR during the first part of the simulations, due to the relatively low biomass compartments, and it cannot reach the high RR response (Fig. 8b) at the end of the simulation.

Total nitrogen (Fig. 8c) shows at the beginning a negative step because of the less biomass injected in FR and AR as initial conditions of the simulation. In the assimilation run recovery of nearer values to "sea-truth" total nitrogen is partially attained, but with no trend toward convergence. A related conclusion is that a sequence of winter mixing periods is needed for attaining total nitrogen bulk content.

Total nitrogen content loss for the reference run is high, about 1300×10^3 ton N year^{-1}. This net unbalance is due to the inflow at Gibraltar of the Atlantic Water and the outflow of the nutrient-rich Lewantine Water, with no positive terrestrial or atmospheric

apports taken into account in the present version of the NPZD ecomodel.

As a matter of fact, the fluxes obtained through various methods with yearly average statistical approach, i.e. inflowing nutrients minus outflowing ones, give estimations from about 2500×10^3 ton N year^{-1} (Lacombe, 1971; Bethoux, 1979) to around half this value (Sarmiento et al., 1988; Bryden and Kinder, 1991; Harzallah et al., 1993). The value previously obtained by NPZD Mediterranean model is thus consistent with the informations and elaborations from existing datasets.

On the other hand, inorganic nitrogen and fractionated nitrogen input runs show very close values in the total nitrogen losses, with simulated atmospheric and terrestrial inputs; in the frame of MFSTEP Project it has been demonstrated that the loss of the total nitrogen budget in the entire Mediterranean Sea is about 28×10^3 ton N year^{-1} for both input runs (Crispi and Pacciaroni, 2005). This picture is obviously affected by uncertainties of the loads, but it is relevant to note that new estimations based upon recent data, from independent sources, are well in line with those considered as inputs of the MFSTEP study.

According with Raicich and Rampazzo (2003), it is possible to evaluate in an OSSE experiment, how much assimilation is important with respect to the free run. Here we want to see the effects of the assimilation on the wrong phytoplankton pre-conditioned ecosystem.

Considering the assimilated, the free and the reference biochemical tracer data, squared standard deviations can be achieved. Their expressions are:

$$\sigma^2_{AR} = \frac{\sum_i (A'_i - R'_i)^2 \cdot \mathrm{Vol}_i}{\sum_i \mathrm{Vol}_i}$$

$$\sigma^2_{FR} = \frac{\sum_i (F'_i - R'_i)^2 \cdot \mathrm{Vol}_i}{\sum_i \mathrm{Vol}_i}$$

where $A'_i = A_i - m_A$, $R'_i = R_i - m_A$, $F'_i = F_i - m_F$ and the squared relative error is:

$$\sigma^2_{AR/FR} = \frac{\sigma^2_{AR}}{\sigma^2_{FR}}$$

in which i are the grid points (363 in longitude, 113 in latitude, 31 in depth); A_i, R_i, F_i are the biochemical tracer concentrations at each grid point, respectively assimilated, reference and free run; m_A, m_R, m_F are their averages; Vol_i is the volume of each cell i.

As a statistical remark, it is worth noting here that the differences between the above expressions and the analogous ones, calculated with their specific anomalies, differ relatively less than 1%.

The above expressions are calculated each of the sixty-nine days of the evolution discriminating three cases: the first range (R1) starts at surface and ends at 20 m depth, the second one spans from 20 m to 4000 m (R2), the third one from surface to 4000 m (R3).

Figure 9 gives the evolution of the phytoplankton relative errors in R1, R2 and R3; the ordinates represent the assimilated run error to the free one ratio, so that a good forecasting index lays below one. The better increase of the assimilation error versus the free error is in the 0–20 m evolution. This is stepwise with oscillations around the 0.5 value, with approximately 50% better error at the end of the sixty-nine days. The error trend of the phytoplankton in R2 is also good with final results of 0.6, with a result slightly worse than the all column relative error.

Figure 10 gives zooplankton relative errors. As expected, zooplankton relative errors remain the same in all the three chosen spatial partitions, approximately 0.7 at the end of the integration period. This value is also reached from inorganic nitrogen in the 0–20 m layer (Fig. 11); while R2 and R3 are practically not affected along all the integration, reaching values around 0.9. Detritus (Fig. 12) has initially a behaviour lower in the case of the 0–20 m with respect to the other two cases, while at the end of the sixty-nine days all the three errors reach slightly higher than 0.6 values.

The total nitrogen error ratios are shown in Fig. 13, indicating striking differences among the deeper layers and the upper 20 m, where the biomass assimilation is performed. In the R2 and R3 ratios, the values are very close to one with small oscillations when phytoplankton is assimilated and with a recovery of the free situation after each assimilation cycle. In the upper layer, the situation tends instead toward a clear decreasing of the assimilation relative error at the beginning, but after four weeks AR exhibits increased relative errors and after six cycles of assimilation the ratio becomes greater than one – thus with assimilation error greater than in free run. The estimates of the nitrogen in all its forms worsen in the case of few weeks biomass univariate assimilation, i.e. not only the forecasting is unfavourable but also deteriorates at last.

This anomaly is not evident at an overall basin scale. The R1 total nitrogen of the assimilated scheme is always between the reference and the free run, indicating a better forecasting average (Fig. 14). This suggests focussing to local effects for understanding what is happening in the layer where the biomass is assimilated.

A different behaviour emerges discussing the R1 average total nitrogen specific contents in the western basin (Fig. 15a) and in the eastern one (Fig. 15b). This is the signature in concentration of the deteriorating effects of the assimilation univariate scheme. There are evident improvements of the total contents after the first three assimilation cycles in both cases; on the other hand, the FR total nitrogen reaches and overcomes that in the AR, only in the western basin during the last month of the simulation, but it remains well below in the eastern side. Moreover the twin numerical experiments cannot reach in this surface layer the reference, winter pre-conditioned, higher total nitrogen contents.

Figure 16 analyses the total nitrogen relative errors in the R1, upper layer. All Mediterranean statistics, as given previously in Fig. 13, shows that this error becomes greater than one, indicating worse forecasting skill of simulation scheme. In the sub-basin evaluations, it is worth noting the presence of the increased error after the fourth cycle of the assimilation (Fig. 16a). Moreover the Western Mediterranean adversely acts in the forecasting: in fact the relative error reaches values well above 1.5. Oth-

erwise the eastern basin (Fig. 16b) shows, even in presence of an increased relative error after the fifth assimilation cycle, no deterioration of the forecasting.

The Western Mediterranean is depicted as an intermediate complexity ecosystem. It contains high phytoplankton biomass with an important, four times less in nitrogen units than that, influence of the zooplankton. Therefore this regime produces high detritus export due to the sloppy feeding, which has time constant about one day, and due to the zooplankton specific mortality, with a five days rate. The Eastern Mediterranean can instead be defined as a phytoplankton-dominated ecosystem. In fact, zooplankton is, in the twin runs, about fifteen times less than phytoplankton biomass. Thus less production of sinking detritus is here present, in any case with a particulate generation time of about 20 days.

5 Conclusions

A three-dimensional coupled physical-biochemical model of the Mediterranean Sea, consisting in GCM evolution of the winter bloom ecosystem variability, has been used in a twin experiment process study for testing a generic reduced-order optimal interpolation data assimilation method. Surface biomass data have been assimilated through SOFA at two quotas, 5 m and 15 m, as constraints of the trophic cycle freely simulated by NPZD description.

As main result, these surface biomass constraints successfully drive phytoplankton concentrations toward better forecasting. Surface biomass takes about 1 month to reach season correct values, starting from wrong summer initial conditions. There is a strong influence on phytoplankton error decrease not only in the top 20 m, where biomass is assimilated, but also in the euphotic area. The relative error, assimilation run versus free run, is about 0.6.

Root mean deviations are generally smaller in the assimilation run than in the free run, for all the four biochemical variables. Inorganic nitrogen exhibits clear improvement at surface, while in the interior the relative error remains about 0.95. Correction of the

biomass in the surface layer is able to influence the concentrations in deeper layers via turbulent mixing processes; on the other hand, it prevents propagation of the surface signals to the deeper layers when the water column is stratified, in the spring, summer and early autumn seasons. Assimilation cycles in successive years would thus be necessary in this framework to recover the euphotic and deeper layer total nitrogen concentrations.

As an exception, the total nitrogen shows a deteriorating relative error in the first 20 m. Such behaviour is completely due to the Western Mediterranean trophic cycling, exporting more detritus from the surface layers. The regional analysis suggests that the present univariate approach aids in improving total nitrogen forecasting in phytoplankton dominated ecosystems, like the Eastern Mediterranean. In presence of more complex interactions with the higher trophic levels, other assimilation strategies, possibly multivariate methodologies, should be proposed and verified in realistic basin scale experiments.

Acknowledgements. This work has been supported by Mediterranean Forecasting System: Toward Environmental Predictions, E. C. Project EVH3-CT-2002-00075.

We wish to thank F. Raicich for his aid at the set-up stage of this work, G. Padoan, for support as computer manager of the ORIGIN 300 at OGS, and S. Calonaci and G. Ballabio, system managers of the SP4 facilities at the Consorzio Interuniversitario del Nord-Est Italiano per il Calcolo Automatico-CINECA.

References

Beers, J. R.: Studies on the chemical composition of the major zooplankton groups in the Sargasso Sea off Bermuda, Limnol. Oceanogr., 11, 520–528, 1966.

Berland, B. R., Benzhitski, A. G., Burlakova, Z. P., Georgieva, L. V., Izmestieva, M. A., Kholodov, V. I., and Maestrini, S. Y.: Conditions hydrologiques estivales en Méditerranée, repartition du phytoplancton et de la matière organique, Oceanol. Acta, 9(SP), 163–177, 1988.

Béthoux, J. P.: Budgets of the Mediterranean Sea. Their dependence on the local climate and on the characteristics of the Atlantic waters, Oceanol. Acta, 2(2), 157–163, 1979.

Bryden, H. and Kinder, T. H.: Steady two-layer exchange through the Strait of Gibraltar, Deep-Sea Res., 38(Suppl. 1), 445–463, 1991.
Civitarese, G., Crise, A., Crispi, G., and Mosetti, R.: Circulation effects on nitrogen dynamics in the Ionian Sea, Oceanol. Acta, 19(6), 609–621, 1996.
Coste, B., Le Corre, P., and Minas, H. J.: Re-evaluation of the nutrient exchanges in the Strait of Gibraltar, Deep-Sea Res., 35, 767–775, 1988.
Crispi G. and Pacciaroni, M.: Towards the nitrate balancing of the Mediterranean Sea: perspective through combination of loads estimate and ecosystem modeling, IMEMS 2005 Proceedings, The 8th International Marine Environmental Modeling Seminar, Helsinki Finland, 23–25 August 2005, 21, 2005.
De May, P. and Benkiran, M.: A Multivariate Reduced-order Optimal Interpolation Method and its Application to the Mediterranean Basin-scale Circulation, in: Ocean Forecasting: conceptual basis and applications, edited by: Pinardi, N. and Woods, J., Springer Verlag, 281–306, 2002.
Demirov, E. and Pinardi, N.: Simulation of the Mediterranean Sea circulation from 1979 to 1993: Part I. The interannual variability, J. Mar. Syst., 33–34, 23–50, 2002.
Eppley, R. W.: Temperature and phytoplankton growth in the sea, Fish. Bull., 70, 1063–1085, 1972.
Harzallah, A., Cadet, D. L., and Crépon, M.: Possible forcing effects of net evaporation, atmospheric pressure, and transients on water transports in the Mediterranean Sea, J. Geophys. Res., 98(C7), 12 341–12 350, 1993.
Lacombe, H.: Le détroit de Gibraltar, océanographie physique, Notes et Mémoires du Service Géologique du Maroc, 222 bis, 111–146, 1971.
Manca, B., Burca, M., Giorgetti, A., Coatanoan, C., Garcia, M.-J., and Iona, A.: Physical and biochemical averaged vertical profiles in the Mediterranean regions: an important tool to trace the climatology of water masses and to validate incoming data from operational oceanography, J. Mar. Syst., 48(1–4), 83–116, 2004.
McGill, D. A.: Mediterranean Sea Atlas – distribution of nutrient chemical properties, Woods Hole Oceanographic Institution, Woodshole, MA, 1970.
Monaco, A. and Peruzzi, S.: The Mediterranean Targeted Project MATER – a multiscale approach of the variability of a marine system – overview, J. Mar. Syst., 33–34, 3–21, 2002.
Osborne, J., Swift, J., and Flinchem, E. P.: OceanAtlas for MacIntosh©, National Science Foundation, 1992.

Pinardi, N., Baretta, J. W., Bianchi, M., Crépon, M., Crise, A., Rassoulzadegan, F., Thingstad, F., and Zavatarelli, M.: Coupled physical-biogeochemical models, in: Interdisciplinary research in the Mediterranean Sea, edited by: Lipiatou, E., EUR 17787, 316–342, 1997.

Raicich, F. and Rampazzo, A.: Observing System Simulation Experiments for the assessment of temperature sampling strategies in the Mediterranean Sea, Ann. Geophys., 21, 151–165, 2003.

Redfield, A. C., Ketchum, B. H., and Richards, F. A.: The influence of Sea Water, in: The Sea, vol. 2, edited by: Hill, M. N., Interscience, New York, 26–77, 1963.

Sarmiento, J. L., Herbert, T., and Toggweiler, J. R.: Mediterranean nutrient balance and episodes of anoxia, Global Biogeochem. Cycles, 2(4), 427–444, 1988.

Sverdrup, H. U., Johnson, M. W., and Fleming, R. H.: The Oceans: their Physics, Chemistry and General Biology, Prentice Hall New York, pp. 1087, 1942.

Zavatarelli, M., Raicich, F., Bregant, D., Russo, A., and Artegiani, A.: Climatological characteristics of the Adriatic Sea, J. Mar. Syst., 18(1–3), 227–263, 1998.

Table 1. List of the biochemical parameters.

Parameter	Definition	Value
η	Zooplankton efficiency	0.75
α	Degradation fraction	0.33
γ	Zooplankton growth	$1.157\times10^{-5}\,s^{-1}$
δ	Zooplankton mortality	$1.730\times10^{-6}\,s^{-1}$
k_P	Grazing half-saturation	$1.0\,\mu mol\ N\ dm^{-3}$
r	Detritus remineralization rate	$1.18\times10^{-6}\,s^{-1}$
k_N	Nitrate half-saturation	$0.25\,\mu mol\ N\ dm^{-3}$
G_{max}	Maximum growth rate	$6.83\times10^{-6}\,s^{-1}$
k_T	Temperature coefficient	$6.33\times10^{-2}{}^{\circ}C^{-1}$
d	Phytoplankton mortality	$5.55\times10^{-7}\,s^{-1}$
K_H	Horizontal turbulent diffusion	$1.5\times10^{18}\,cm^4\,s^{-1}$
K_V	Vertical turbulent diffusion	$1.5\,cm^2\,s^{-1}$
k_z	Light extinction coefficient	$0.00034\,cm^{-1}$
I_{opt}/I_0	Otimum light ratio	0.5
n_C	Cox turbulence iteration number	10
α_{BT}	Newtonian restoration time	$1.0\ day^{-1}$
w_{BT}	Sinking for the N, P, Z, D tracers	$0, 0, 0, 0.0058\,cm\,s^{-1}$

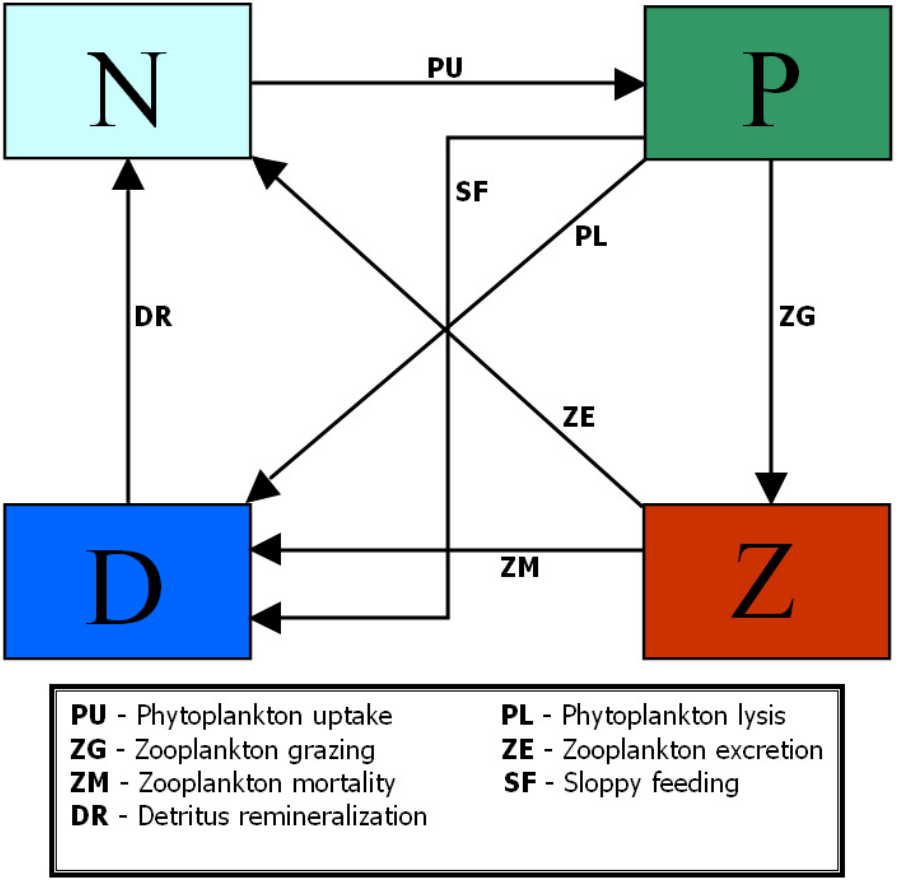

Fig. 1. Diagram of the nitrogen fluxes linking the biochemical compartments NPZD.

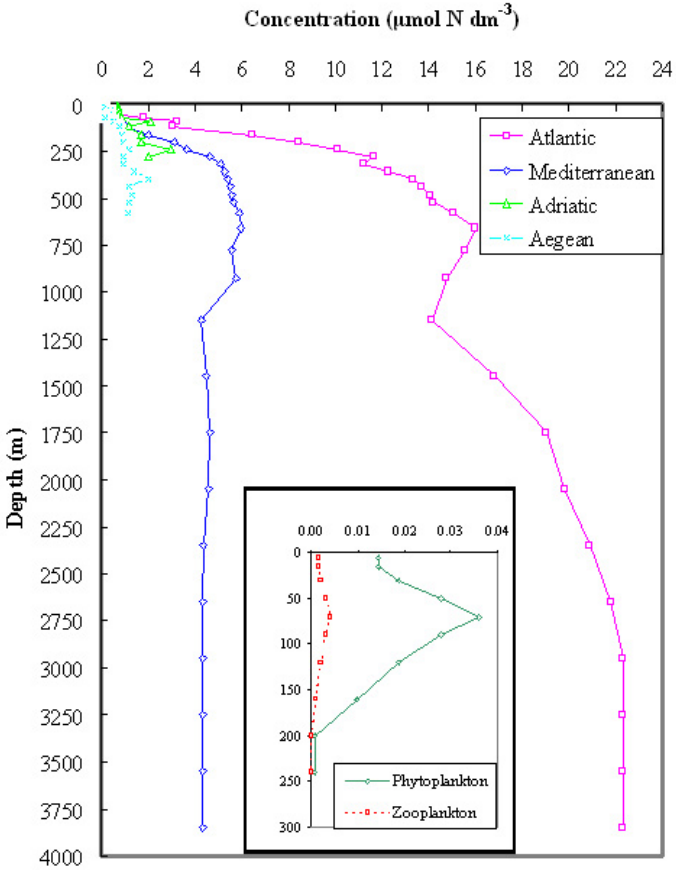

Fig. 2. Inorganic nitrogen initial vertical profile in the Mediterranean Sea and inorganic nitrogen restoration profiles in the Atlantic buffer box and in the Adriatic and Aegean marginal seas. Phytoplankton and zooplankton initial profiles are given in the inner plate with the same units (μmol N dm^{-3}).

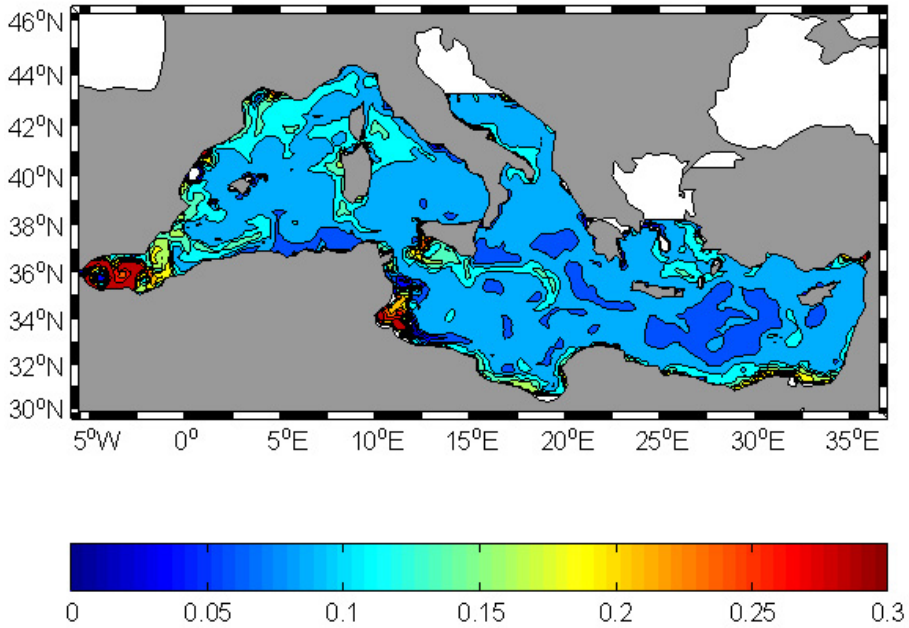

Fig. 3. Average phytoplankton concentrations (μmol N dm^{-3}) after 60 days.

OSD
3, 503–539, 2006

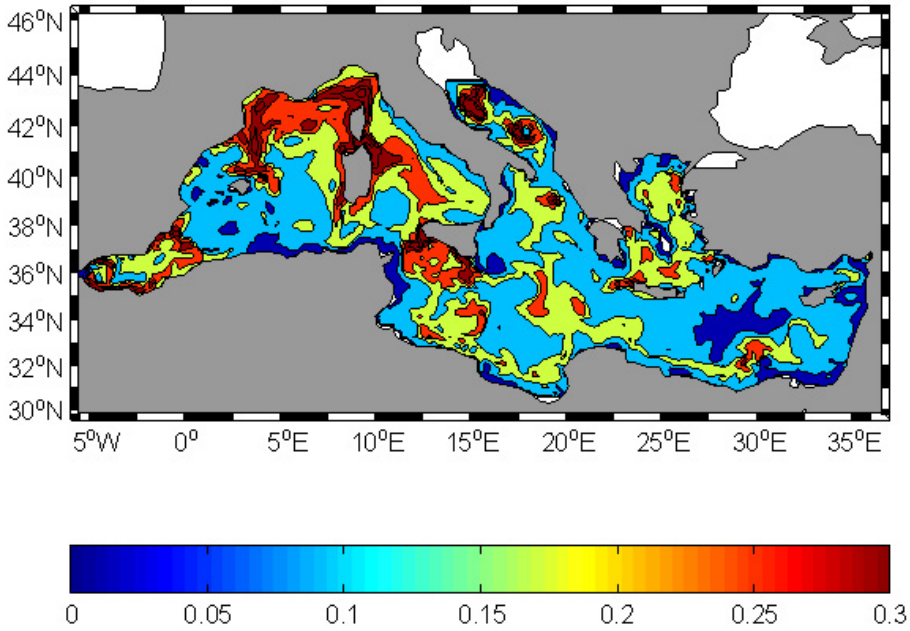

Fig. 4. Average surface phytoplankton concentrations (μmol N dm^{-3}) after 120 days.

OSD
3, 503–539, 2006

EGU

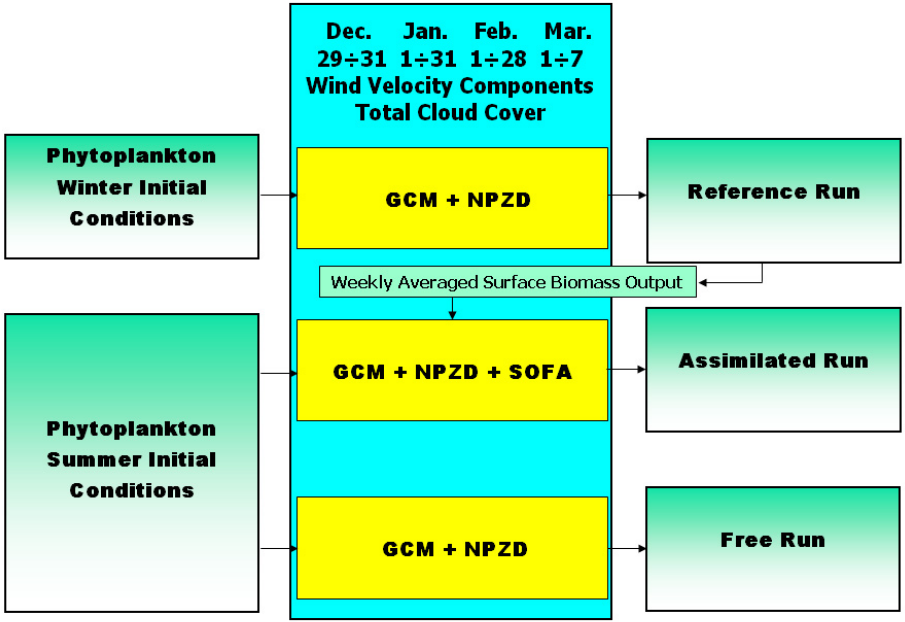

Fig. 5. OSSE strategy and assimilated data generator. The GCM physical variability spans in the twin numerical experiments the same period from 29 December to 7 March using u and v wind velocity components and total cloud coverage, and turning the winter conditions of the phytoplankton into summer initial values.

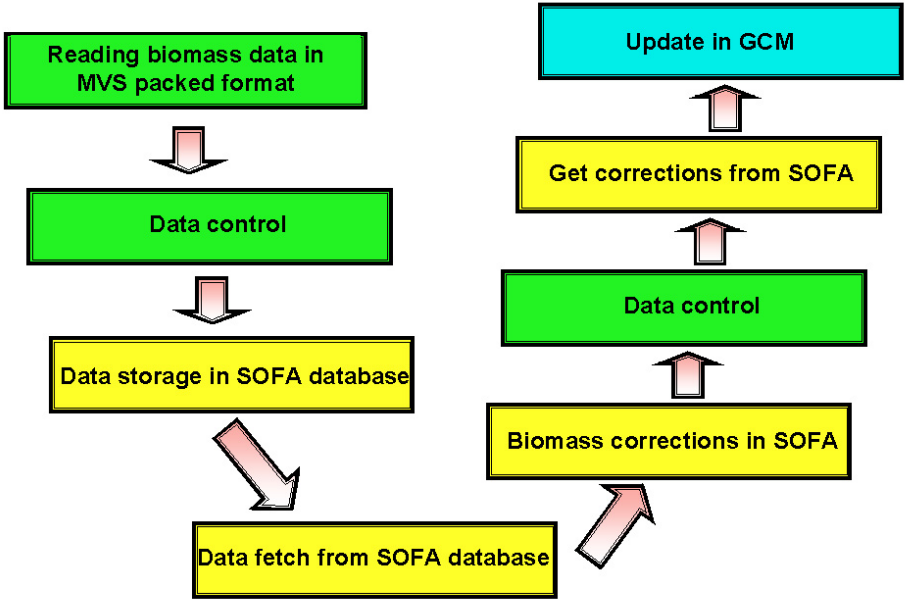

Fig. 6. Data flow SOFA/GCM: reading data to be assimilated, calculating corrections in SOFA and updating in GCM.

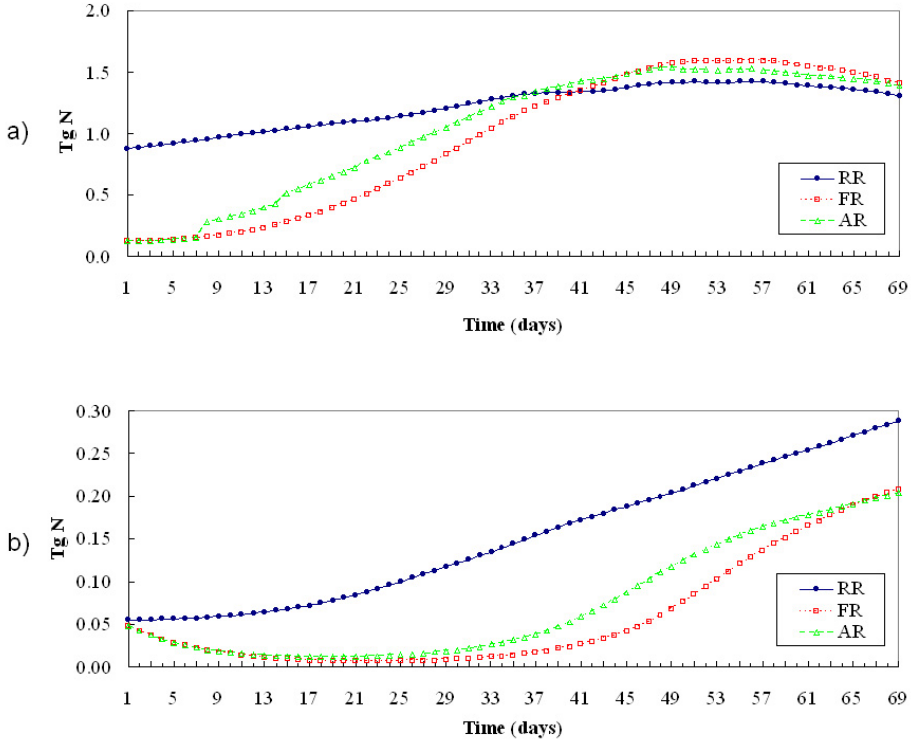

Fig. 7. Basin average phytoplankton **(a)** and zooplankton **(b)** evolutions along the 69 days of the RR, FR and AR in 10^{12} g N (Tg N).

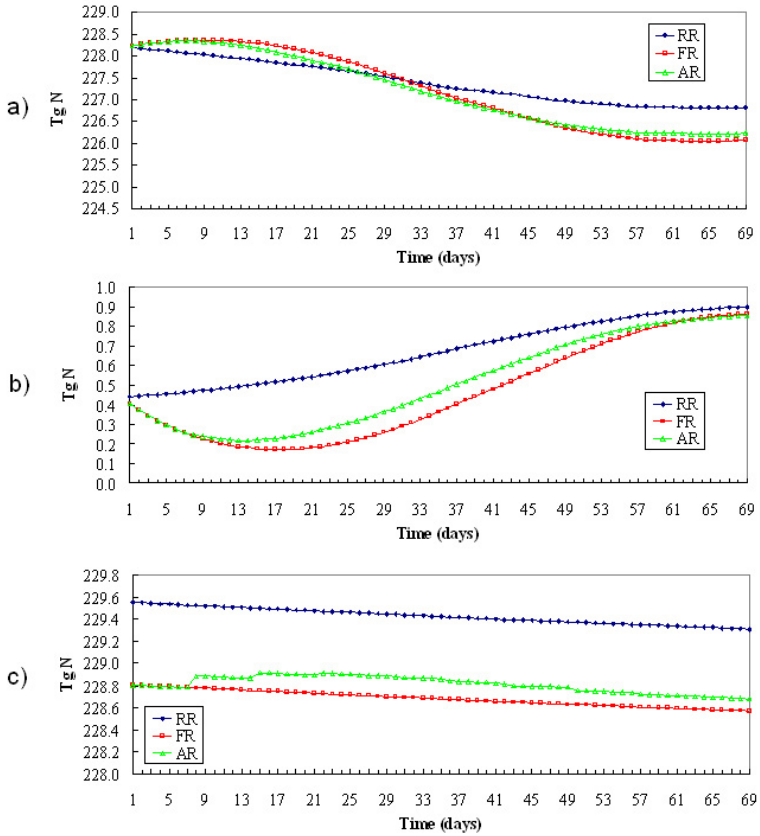

Fig. 8. Basin average inorganic nitrogen **(a)**, detritus **(b)** and total nitrogen **(c)** evolutions along the 69 days of the RR, FR, AR in 10^{12} g N (Tg N).

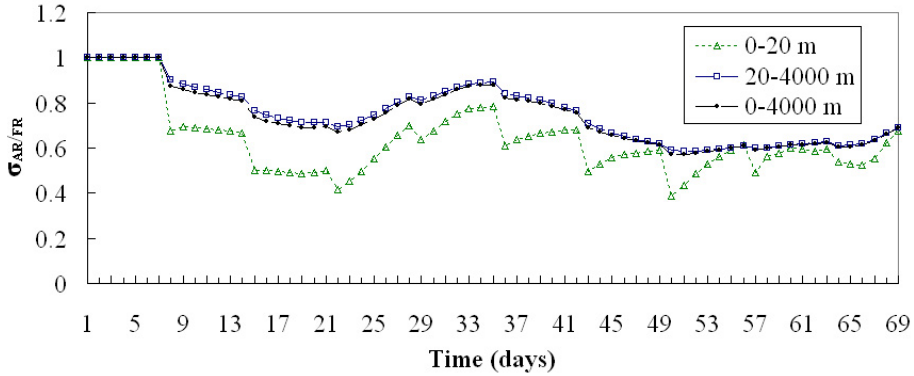

Fig. 9. Phytoplankton relative errors in R1 (0–20 m), R2 (20–4000 m) and R3 (0–4000 m).

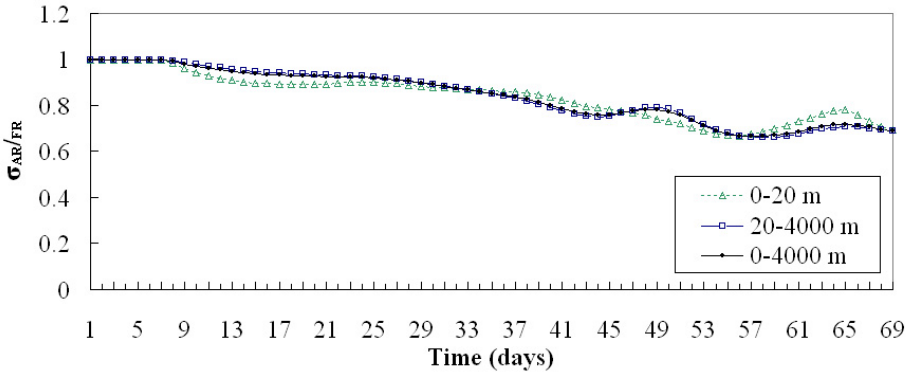

Fig. 10. Zooplankton relative errors in R1, R2, and R3.

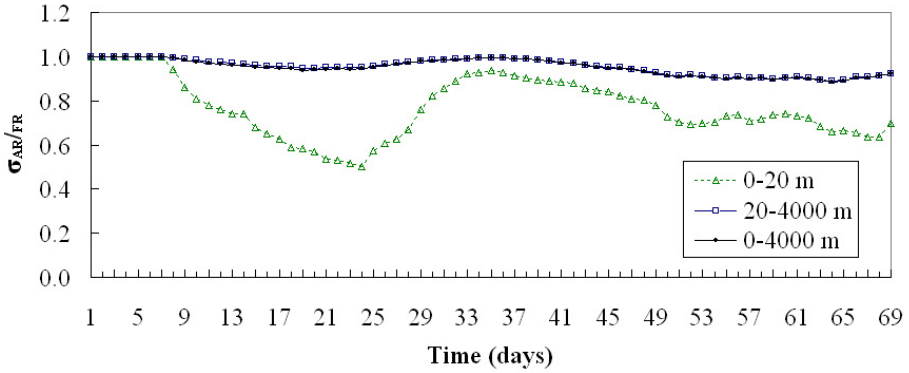

Fig. 11. Inorganic nitrogen relative errors in R1, R2 and R3.

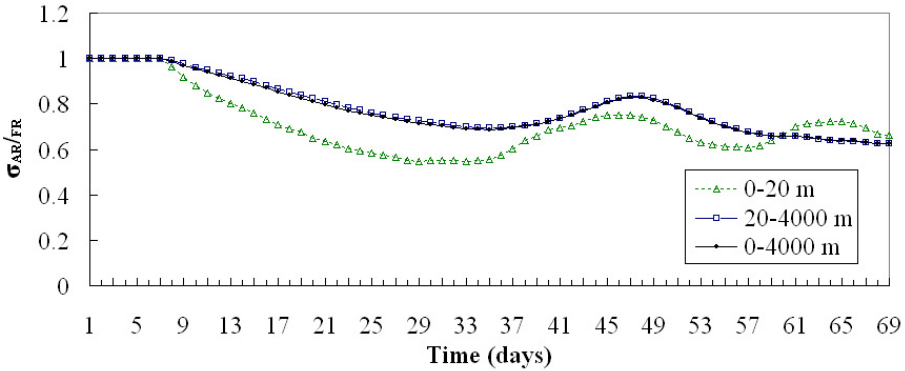

Fig. 12. Detritus relative errors in R1, R2 and R3.

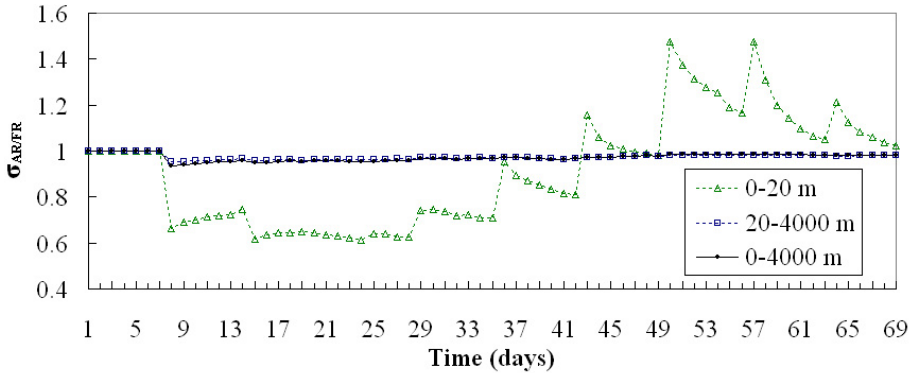

Fig. 13. Total nitrogen relative errors in R1, R2 and R3.

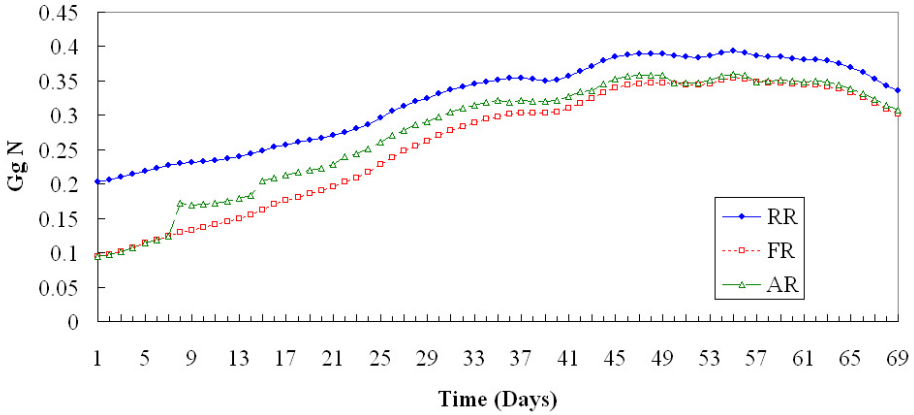

Fig. 14. Upper layer (0–20 m) Mediterranean total nitrogen content in 10^9 g N (Gg N) for RR, FR and AR.

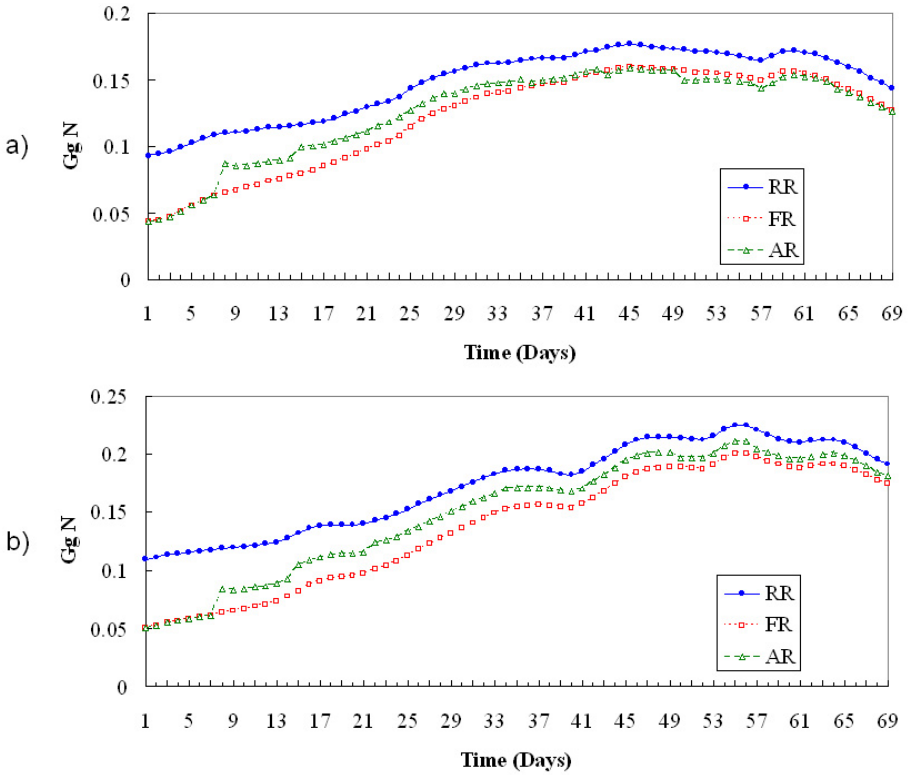

Fig. 15. R1 (0–20 m) total nitrogen content in the western **(a)** and eastern basins **(b)** expressed in 10^9 g N (Gg N) for RR, FR and AR.

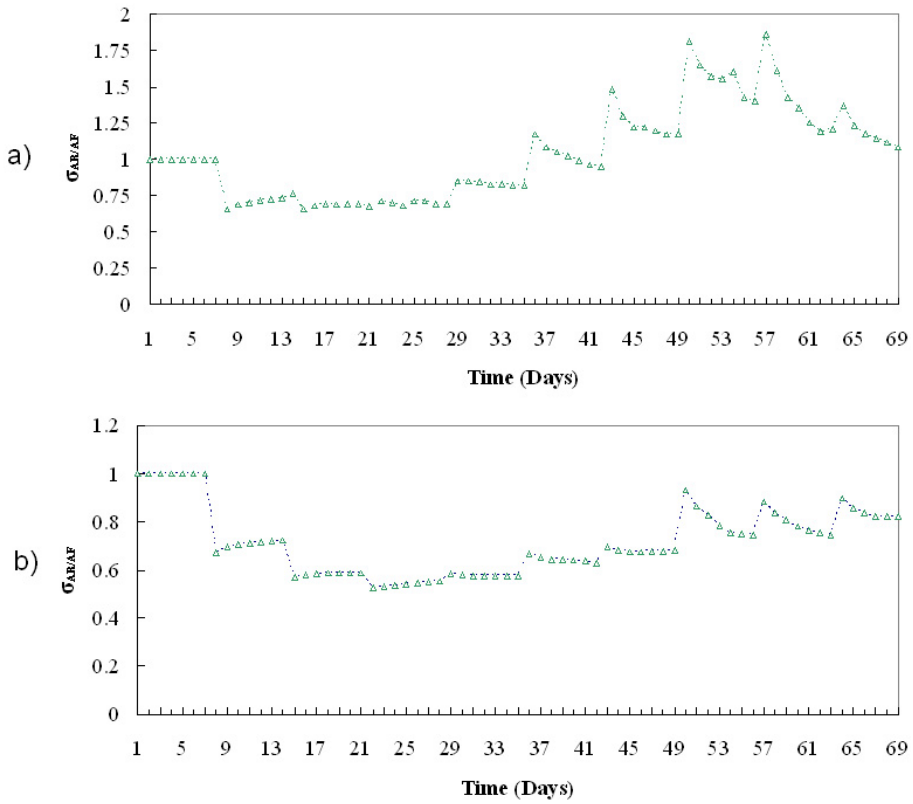

Fig. 16. R1 (0–20 m) total nitrogen relative errors in the western **(a)** and eastern basins **(b)**.